Available online at www.sciencedirect.com
ScienceDirect
Journal of Power Sources 158 (2006) 1442–1446
JOURNAL OF POWER SOURCES
www.elsevier.com/locate/jpowsour

Short communication

# A spin-coated solid polymer electrolyte for all-solid-state rechargeable thin-film lithium polymer batteries

Cheol-Ho Park *, Min Park, Sang-Im Yoo, Seung-Ki Joo

*School of Materials Science and Engineering, Seoul National University, Seoul 151-742, South Korea*

Received 6 September 2005; received in revised form 4 October 2005; accepted 4 October 2005
Available online 23 November 2005

**Abstract**

This paper proposes a new approach of using a spin-coated solid polymer electrolyte in the fabrication of an all-solid-state rechargeable thin-film lithium battery with the cell structure of Li/polymer/$LiMn_2O_4$. Room temperature cycling of this cell showed comparable cycling performance and good Coulombic efficiency at the 6 C rate (100 $\mu A\,cm^{-2}$). On removing the spin-coated solid polymer electrolyte after the cycle test, we observed a morphology change on the $LiMn_2O_4$ cathode surface using a field emission scanning electron microscope (FE-SEM). FE-SEM also showed that there had been dissolution/precipitation of manganese species at the cathode/electrolyte interface during cycles.


*Keywords:* Solid polymer electrolyte; Spin-coating; Rechargeable thin-film battery; Manganese species

## 1. Introduction

Since Bates et al. [1] reported a rechargeable thin-film lithium battery a decade ago, many researchers have engaged in efforts to develop thin-film batteries (TFBs). TFBs could be potentially applied to microelectronic mechanical systems (MEMSs), implantable medical devices, integrated circuits with self-power sources, smart cards, and portable electronic devices [2]. Many types of TFB and TFB fabrication techniques have been reported [1–7]. Most of these TFB types were based on amorphous inorganic electrolytes, such as lithium–phosphorus oxynitride (Lipon) [1,2], $Li_2O$–$V_2O_5$–$SiO_2$ [4,5], $Li_{1.9}Si_{0.28}P_{1.0}O_{1.1}N_{1.0}$ (LISIPON) [7], lithium–sulfur oxynitride (Lison) [8], etc. In order to deposit an electrolyte film several micrometers-thick, researchers have used conventional thin-film fabrication techniques, for example: radio-frequency reactive magnetron sputtering [1–6,8], pulsed laser deposition [9], ion beam assisted deposition [10], etc. While it is known that exact stoichiometric control is the most critical factor in obtaining ideal electrolyte properties, this is not easy to implement and requires that the same operating conditions are maintained from batch to batch.

On the other hand, in the case of the 'bulk' battery, many researchers have attempted to fabricate all-solid-state lithium polymer batteries (LPBs) using solid polymer electrolytes (SPEs) [11–15]. Unlike the gel-type polymer lithium ion batteries, all-solid-state LPBs ensure safety since they do not involve the use of highly volatile liquids, but still achieve a high energy density using metallic lithium [11,12]. The vast majority of these all-solid-state LPBs were fabricated by sandwiching the SPE between a lithium anode and a composite cathode. However, the low ionic conductivity of thick SPE and the poor interface characteristics between the electrodes and the polymer electrolyte are the main problems that prevent these all-solid-state LPBs from being manufactured [16].

In this paper, we propose a new approach of using SPE to fabricate an all-solid-state rechargeable thin-film lithium battery. We spin-coated the polymer electrolyte directly onto a thin-film $LiMn_2O_4$ cathode and then deposited a thin-film lithium anode onto it by conventional vacuum evaporation. By using an easy and simple spin-coating method, a SPE film with a thickness of 20–30 $\mu$m can be formed. This is thin enough to facilitate Li ion conduction because the ionic conductivity of our SPE is about $10^{-4}\,S\,cm^{-1}$, which is two orders of magnitude higher than that of Lipon, about $10^{-6}\,S\,cm^{-1}$ [17]. We anticipated that there would be a good interface between the spin-coated SPE and the cathode film due to the absence of the detached area that is usually formed in the general solid/solid sandwiching method.

* Corresponding author. Tel.: +82 2 880 7442; fax: +82 2 887 8791.
*E-mail address:* chpark00@snu.ac.kr (C.-H. Park).

0378-7753/$ – see front matter © 2005 Elsevier B.V. All rights reserved.
doi:10.1016/j.jpowsour.2005.10.022

Because the polymer electrolyte was spin-coated and dried directly on the cathode film, the cathode/electrolyte interface had better adhesion than the sandwiched solid/solid interface. The evaporation method also yielded a contamination-free interface between lithium and SPE with good adhesion. We not only investigated the electrochemical characteristics of our thin-film LPB, but also observed the morphology change of cathode film after the cycle test owing to the fact that with a proper solvent, it is possible to remove the SPE film easily.

## 2. Experimental

The thin-film cathode samples were deposited from a 5.08 cm $LiMn_2O_4$ ceramic target by radio-frequency magnetron sputtering on a Pt (200 nm)/$TiO_2$ (10 nm)/$SiO_2$/Si wafer. The Pt layer served as a current collector and the $TiO_2$ layer was deposited for good adhesion between the Pt and $SiO_2$ layer. The $LiMn_2O_4$ target was fabricated in house from $LiMn_2O_4$ powder (Aldrich), which was cold pressed and annealed at 1000 °C for 5 h in air. Films of 0.2–0.3 μm thick were deposited at the rate of 3–10 Å $min^{-1}$ in $Ar + O_2$ processing gas. The processing pressure was 10 mTorr and Ar:$O_2$ mixture ratio was 10:1. The substrates were heated to 300 °C during the deposition. The deposited samples were annealed at 750 °C for 2 h in a furnace with an oxygen atmosphere. The cathode thin-films were characterized by X-ray diffraction (XRD), FE-SEM and charge–discharge cycling of a half-cell with a lithium metal anode and a liquid electrolyte. The liquid electrolyte was 1 M of $LiPF_6$ in ethylene carbonate (EC)/diethyl carbonate (DEC) (1/2, v/v) provided by Samsung Cheil Industries Inc.

The SPE was obtained by combining poly(ethylene oxide) (PEO, Aldrich, molecular weight = 1,000,000 g) with $LiClO_4$ (Aldrich). The PEO/$LiClO_4$ concentration ratio was 18/1. The SPE was prepared according to the following procedures. First, a proper amount of $LiClO_4$ was dispersed in acetonitrile, and then PEO polymer component was added. Next, the mixture was stirred for 3 days at 70 °C into the resulting slurry. We controlled the viscosity of the slurry by evaporating some amounts of acetonitrile. The slurry was spin-coated onto the cathode films and the solvent was allowed to evaporate in an argon-filled dry box for 24 h at room temperature. The spin-coated films were dried under vacuum for another 5 h at room temperature. The typical spin speed was about 3000–5000 revolutions per minute (rpm). These procedures yielded SPE films with a thickness of 25–30 μm, according to the viscosity of the slurry and the spin speed.

After the SPE films were produced, a lithium metal film was deposited onto the spin-coated SPE by the conventional thermal evaporation. To form an electrical contact to the Pt layer, we removed an edge part of SPE film with a razor blade. The rough sketch of the cell structure is shown in Fig. 1.

The TFB was cycled in an argon-filled dry box with WBCS3000 (WonATech), battery cycler system. We charged the battery to 4.4 V at a constant current density of 100 μA $cm^{-2}$, held it at this potential for 1 min and then discharged it at the same current density until the cell voltage reached 3.3 V. The electrochemical impedance characteristics of the TFB were measured

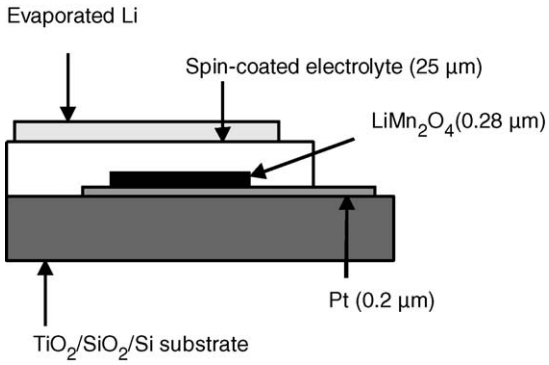


Fig. 1. Schematic cross section of a thin-film lithium polymer battery.

in the frequency range of 10 and 2 MHz at the open circuit voltage of 4.0 V with IM5d (Zahner) system at room temperature.

In order to observe the surface morphology of $LiMn_2O_4$ film with FE-SEM after the cycle test, the lithium and the SPE films in the TFB were removed by washing with acetonitrile.

## 3. Results and discussion

Fig. 2 shows the XRD scan for deposited $LiMn_2O_4$ cathode film after being annealed in a furnace at 750 °C for 2 h. This XRD pattern of annealed film matches the JCPDS file for $LiMn_2O_4$ (no. 35-0782) and shows good crystallinity. Fig. 3 shows the FE-SEM image of deposited $LiMn_2O_4$ film (a) before and (b) after the furnace annealing. Fig. 3(a) illustrates partially crystallized $LiMn_2O_4$ grains that must have grown at the deposition step due to the heating of the substrate to 300 °C. The average size of grains was initially about 70 nm but can be seen to have grown to an average size of 80 nm after annealing. The grain boundaries became more distinct after the furnace annealing as seen in Fig. 3(b).

Fig. 4(a) shows the room-temperature charge–discharge curves of the cathode film with a liquid electrolyte and a lithium metal anode. The half-cell was cycled at a current density of 100 μA $cm^{-2}$, which is equivalent to the 6 C rate,

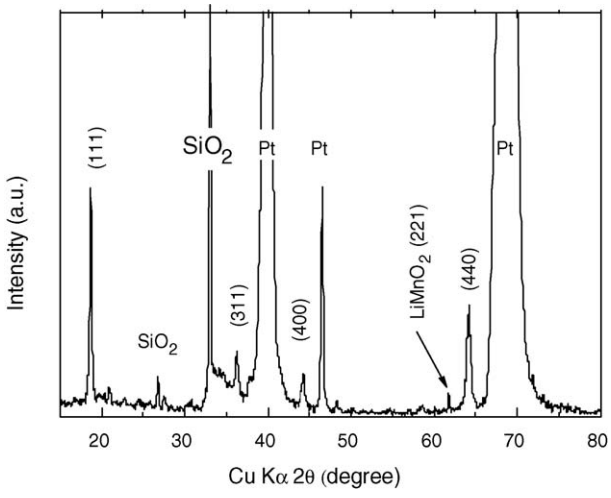


Fig. 2. X-ray diffraction pattern of $LiMn_2O_4$ film.

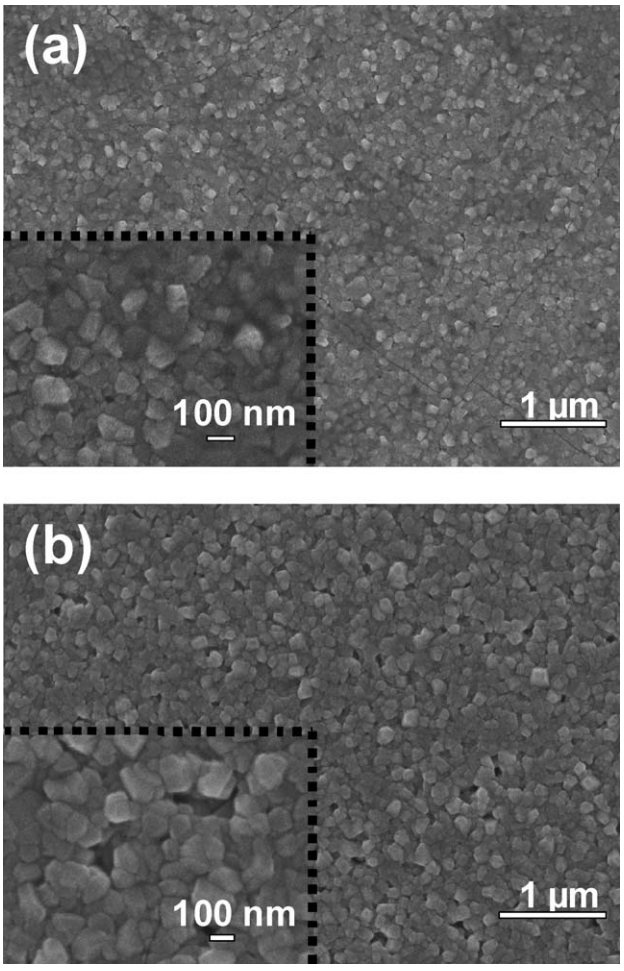


Fig. 3. FE-SEM images of $LiMn_2O_4$ film surface (a) as deposited at 300 °C and (b) after furnace annealing at 750 °C for 2 h in $O_2$ atmosphere.

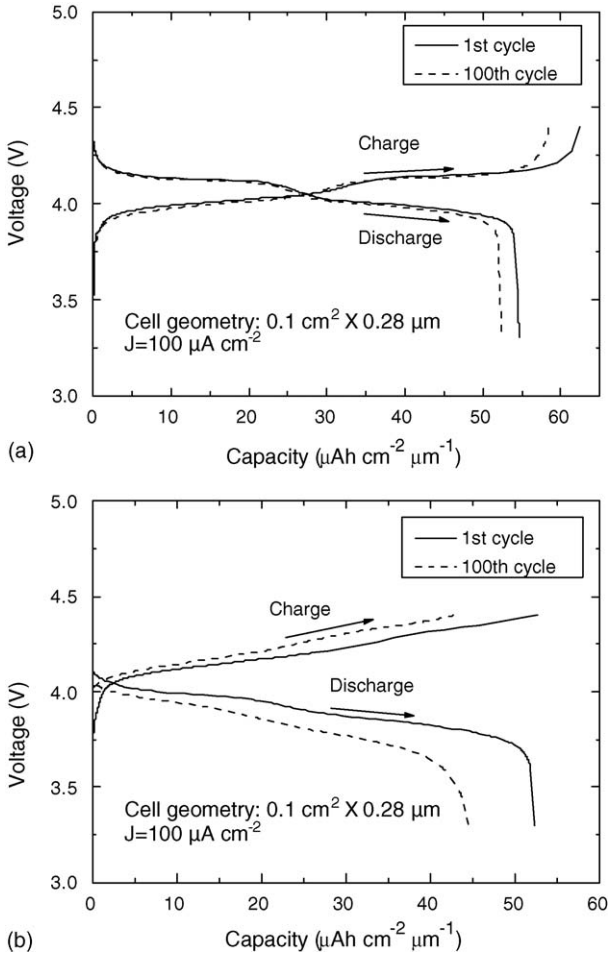


Fig. 4. The charge–discharge characteristics of (a) Li/liquid electrolyte/$LiMn_2O_4$/Pt cell and (b) Li/solid polymer electrolyte/$LiMn_2O_4$/Pt cell, showing the 1st (solid line) and 100th (dashed line) cycle measured at the current density of 100 μA $cm^{-2}$ between 4.4 and 3.3 V.

between 4.4 and 3.3 V. The dimension of the cathode was 2 mm × 5 mm × 0.28 μm. The discharge occurred at a nearly constant potential of 4.12 V and 3.97 V. There was only a capacity loss of 4% up to the 100th cycle and the average Coulombic efficiency was 85%. This excellent cycling performance indicates that our cathode samples were well fabricated.

Fig. 4(b) shows the room-temperature electrochemical behavior of the all-solid-state rechargeable thin-film Li/polymer/$LiMn_2O_4$ battery. The TFB was cycled under the same conditions as the liquid cell in Fig. 4(a). The first discharging capacity was 53 μAh $cm^{-2}$ $\mu m^{-1}$, which corresponds to 0.83 Li per mole of $Mn_2O_4$. The discharge capacity of the cell decreased slowly to 85% of the initial capacity by the 100th cycle. The average Coulombic efficiency was 93%, which is much higher than that of the liquid electrolyte. This shows that the spin-coated SPE is electrochemically more stable than the liquid electrolyte.

Fig. 5 shows the Nyquist plot of the solid cell after the 1st cycle and the 100th cycle at the open circuit voltage of 4.0 V. By using the impedance data, we calculated the ionic conductivity ($\sigma$) of the spin-coated SPE. It was calculated from $\sigma = (1/R) \times (d/A)$, where $d$ and $A$ are the thickness of the polymer electrolyte and the area of the cell, respectively. $R$ is the estimated

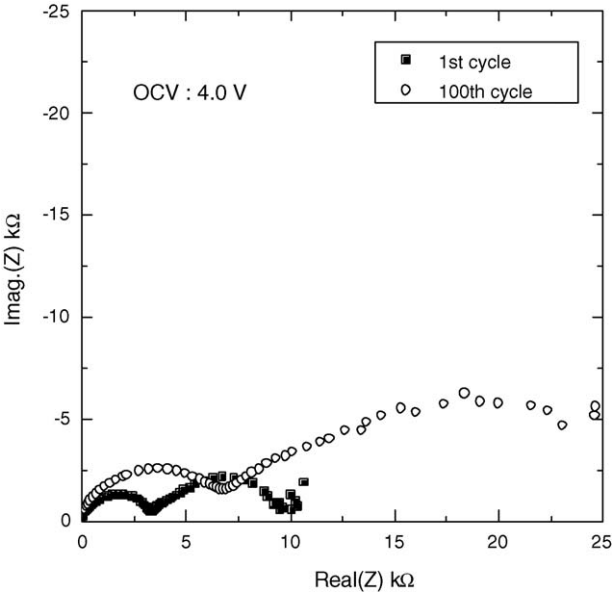


Fig. 5. Nyquist plots obtained from Li/solid polymer electrolyte/$LiMn_2O_4$/Pt cell at open circuit voltage (OCV) of 4.0 V measured after 1st and 100th cycle.

real impedance value, Real($Z$), at the near-infinite frequency, which represents the serial resistance of the typical equivalent circuit [18]. The impedance spectra consist of two arcs in the higher and lower frequency ranges. The arcs may correspond to the reactions at the Li/SPE interface and SPE/$LiMn_2O_4$ interface. While it needs more in-depth measurement and analysis to discern which of the arcs corresponds to the Li/SPE interface and which to the SPE/$LiMn_2O_4$ interface, the increase of both arcs' radius after 100 cycles shows that the interfacial resistances of both interfaces increased during the cycle test. The calculated ionic conductivity, however, remains nearly constant and the value is $1.2 \times 10^{-4}$ S cm$^{-1}$, which is within a relatively high range, compared with the reported conductivity values [19].

Fig. 6(a) shows the FE-SEM image of the $LiMn_2O_4$ surface after 100 cycles in the liquid electrolyte cell. Compared with Fig. 3(b), the average size of grains is reduced to about 60 nm. This proves that manganese ions were dissolved during the cycle as reported [20,21]. Myung et al. [22] even observed the disruption of the spinel $LiMn_2O_4$ particles due to the dissolution of manganese ions, when $Li^+$ ions were inserted into the particles. Fig. 6(a) also shows that the $LiMn_2O_4$ grains connected together to form a big cluster of particles (which is indicated by the arrow and one-dot chain line), implying that there is a re-attachment of manganese species that were previously dissolved during the process of intercalation or deintercalation.

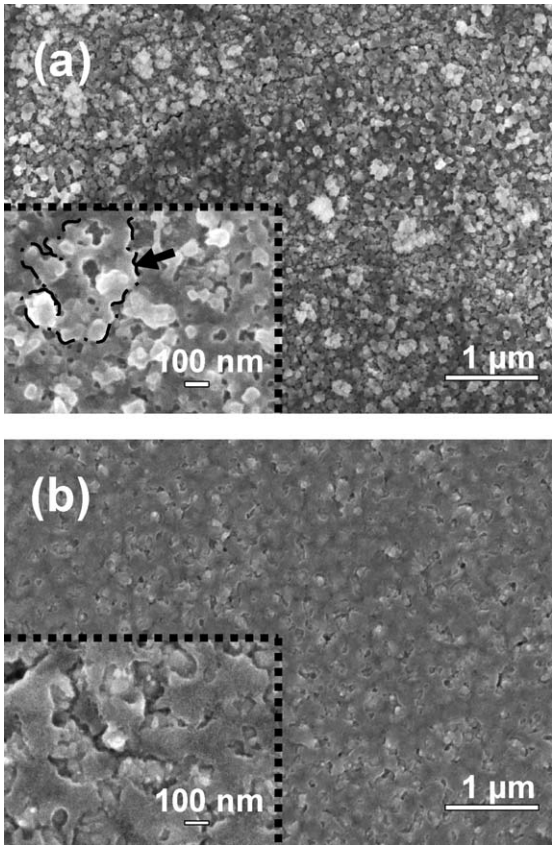


Fig. 6. FE-SEM images of $LiMn_2O_4$ film surface after 100th cycle (a) in Li/liquid electrolyte/$LiMn_2O_4$/Pt cell and (b) in Li/solid polymer electrolyte/$LiMn_2O_4$/Pt cell.

Fig. 6(b) shows the morphology of the $LiMn_2O_4$ surface after 100 cycles in the solid electrolyte cell. The surface is mostly smooth except for some pores through which we can see the underlying grains. All of the grains at the interface between the $LiMn_2O_4$ and the SPE are connected to form one flat cathode. Inaba et al. [23] observed the morphology change of the spinel $LiMn_2O_4$ film by potential cycling in liquid electrolyte with electrochemical scanning tunneling microscopy (STM). They reported that small particles appeared and covered the $LiMn_2O_4$ grains after repeated cycling. They suggested that the newly formed small particles were formed from the liquid solution as a result of a dissolution/precipitation reaction and thus should have less crystallinity or have a composition different from the original $LiMn_2O_4$. Moon et al. [24] also observed the morphology change of thin-film $LiMn_2O_4$ in liquid electrolyte cell after 100 cycles of charge–discharge. Their FE-SEM images show similar results to those of Inaba et al.

In the case of our solid electrolyte cell, the dissolved manganese species could not move out due to the blocking of the SPE and formed a flat precipitation at the interface. This demonstrates the good blocking feature of the SPE film that prevents cathode material loss during cycles. This newly formed interface material, however, is likely to have an amorphous structure, which is inferred by the fact that there was no faceted edge, which is a typical of crystalline material.

It is this amorphous material that causes the increase of interfacial resistance as shown in impedance spectra in Fig. 5. It also explains why there is a larger difference of initial ohmic drop after the 100th cycle in the solid cell than in the liquid cell as seen in Fig. 4.

## 4. Conclusions

In this study, we fabricated an all-solid-state thin-film lithium polymer battery with a PEO based polymer electrolyte. $(PEO)_{18}LiClO_4$ was spin-coated directly onto the thin-film $LiMn_2O_4$ cathode and then lithium was evaporated onto it. The capacity loss was less than 15% after the 100 cycles at a current density of 100 μA cm$^{-2}$, which is equivalent to a 6 C rate. The first discharging capacity was approximately 53 μAh cm$^{-2}$ μm$^{-1}$, which corresponds to 0.83 Li per mole of $Mn_2O_4$. The Coulombic efficiency was 93%, which is much higher than that in a liquid electrolyte. This, in turn, shows that the spin-coated SPE is electrochemically more stable than the liquid electrolyte. FE-SEM images of the cathode film surface that were taken before and after the cycle test show the good blocking feature of the SPE film that prevented cathode material loss during cycles. However, the re-attachment or precipitation of previously dissolved manganese species at the interface caused an increase in interfacial resistance, which is one of the new sources of the capacity fading in the thin-film lithium polymer batteries.

## Acknowledgements

A Korea Research Foundation Grant (KRF-2000-042-E00110) supported this work. The FE-SEM measurements in

this work were done by the National Center For Inter-University Research Facilities, Seoul National University, Korea.

## References

[1] J.B. Bates, N.J. Dudney, D.C. Lubben, G.R. Gruzalski, B.S. Kwak, X. Yu, R.A. Zuhr, J. Power Sources 54 (1995) 58.
[2] J.B. Bates, N.J. Dudney, B. Neudecker, A. Ueda, C.D. Evans, Solid State Ionics 135 (2000) 33.
[3] E.J. Jeon, Y.W. Shin, S.C. Nam, W.I. Cho, Y.S. Yoon, J. Electrochem. Soc. 148 (2001) A318.
[4] S. Zhao, Q. Qin, J. Power Sources 122 (2003) 174.
[5] H. Ohtsuka, Y. Sakurai, Solid State Ionics 144 (2001) 59.
[6] S.-J. Lee, H.-K. Baik, S.-M. Lee, Electrochem. Commun. 5 (2003) 32.
[7] P.E. Trapa, Y.-Y. Won, S.C. Mui, E.A. Olivetti, B. Huang, D.R. Sadoway, A.M. Mayers, S. Dallek, J. Electrochem. Soc. 152 (2005) A1.
[8] K.-H. Joo, H.-J. Sohn, P. Vinatier, B. Pecquenard, A. Levasseur, Electrochem. Solid-State Lett. 7 (2004) A256.
[9] J. Kawamura, N. Kuwata, K. Toribami, N. Sata, O. Kamishima, T. Hattori, Solid State Ionics 175 (2004) 273.
[10] F. Vereda, N. Clay, A. Gerouki, R.B. Goldner, T. Haas, P. Zerigian, J. Power Sources 89 (2000) 201.
[11] M.C. Borghini, M. Mastragostino, A. Zanelli, Electrochim. Acta 41 (1996) 2369.
[12] K.M. Abraham, H.S. Choe, D.M. Pasquariello, Electrochim. Acta 43 (1998) 2399.
[13] Y.-K. Sun, D.-W. Kim, Y.-M. Choi, J. Power Sources 79 (1999) 231.
[14] L. Gao, D.D. Macdonald, M. Urquidi-Macdonald, D.L. Olmeijer, H.R. Allcock, Electrochim. Acta 47 (2002) 3863.
[15] Y. Kobayashi, H. Miyashiro, T. Takeuchi, H. Shigemura, N. Balakrishnan, M. Tabuchi, H. Kageyama, T. Iwahori, Solid State Ionics 152/153 (2002) 137.
[16] Y. Xia, T. Fujieda, K. Tatsumi, P.P. Prosini, T. Sakai, J. Power Sources 92 (2001) 234.
[17] X. Yu, J.B. Bates, G.E. Jellison Jr., F.X. Hart, J. Electrochem. Soc. 144 (1997) 524.
[18] J. Fan, P.S. Fedkiw, J. Power Sources 72 (1998) 165.
[19] B.-K. Choi, Y.-W. Kim, Electrochim. Acta 49 (2004) 2307.
[20] D.H. Jang, Y.J. Shin, S.M. Oh, J. Electrochem. Soc. 143 (1996) 2204.
[21] Y. Xia, Y. Zhou, M. Yoshio, J. Electrochem. Soc. 144 (1997) 2593.
[22] S.-T. Myung, H.-T. Chung, S. Komaba, N. Kumagai, H.-B. Gu, J. Power Sources 90 (2000) 103.
[23] M. Inaba, T. Doi, Y. Iriyama, T. Abe, Z. Ogumi, J. Power Sources 81/82 (1999) 554.
[24] H.-S. Moon, W. Lee, P.J. Reucroft, J.-W. Park, J. Power Sources 119–121 (2003) 710.